Defining a novel *cis* element in the 3'-untranslated region of mammalian ribonucleotide reductase component R2 mRNA: role in transforming growth factor-β₁ induced mRNA stabilization

Francis M. Amara, Frank Y. Chen and Jim A. Wright*

Manitoba Institute of Cell Biology and Department of Biochemistry and Molecular Biology, University of Manitoba, 100 Olivia Street, Winnipeg, Manitoba R3E 0V9, Canada

ABSTRACT

Ribonucleotide reductase R2 gene expression is elevated in BALB/c 3T3 fibroblasts treated with transforming growth factor β₁. We investigated the possibility that the 3'-UTR of ribonucleotide reductase R2 mRNA contains regulatory information for TGF-β₁ induced message stability. Using end-labeled RNA fragments in gel shift assays and UV cross-linking analyses, we detected in the 3'-UTR a novel 9 nucleotide (nt) *cis* element, 5'-GAGUUUGAG-3' site, which interacted specifically with a cytosolic protease sensitive factor to form a 75 kDa complex. The *cis* element protein binding activity was inducible and markedly up-regulated cross-link 4 h after TGF-β₁ treatment of mouse BALB/c 3T3 cells. Other 3'-UTRs [IRE, GM-CSF, c-*myc* and homopolymer (U)] were poor competitors to the *cis* element with regard to forming the TGF-β₁ dependent RNA–protein complex. However, the *cis* element effectively competed out the formation of the R2 3'-UTR protein complex. Cytosolic extracts from a variety of mammalian cell lines (monkey Cos7, several mouse fibrosarcomas and human HeLa S3) demonstrated similar TGF-β₁ dependent RNA–protein band shifts as cell extract from BALB/c 3T3 mouse fibroblasts. Binding was completely prevented by several different mutations within the *cis* element, and by substitution mutagenesis, we were able to predict the consensus sequences, 5'-GAGUUUNNN-3' and 5'-NNNUUUGAG-3' for optimal protein binding. These results support a model in which the 9 nt region functions *in cis* to destabilize R2 mRNA in cells; and upon activation, a TGF-β₁ responsive protein is induced and interacts with the 9 nt *cis* element in a mechanism that leads to stabilization of the mRNA. This appears to be the first example of a mRNA binding site that is involved in TGF-β₁-mediated effects.

INTRODUCTION

Mammalian ribonucleotide reductase is composed of two dissimilar dimeric protein components, proteins R1 and R2, which are required to catalyze the direct reduction of ribonucleoside diphosphates to the corresponding deoxyribonucleotides, a rate limiting step in the synthesis of DNA (1,2). Changes in enzyme activity and R1 and/or R2 gene expression have been observed under a variety of conditions. For example, the expression of the ribonucleotide reductase R1 and R2 genes are induced in BALB/c 3T3 cells by transforming growth factor β₁ (TGF-β₁), and R2 gene expression is abnormally regulated by TGF-β₁ in highly malignant fibrosarcomas (3,4). The importance of ribonucleotide reduction in mechanisms of cell proliferation and DNA repair (4,5), and the findings that regulation of the enzyme is altered in some malignant conditions (6), have made it a target for the development of chemotherapeutic compounds (2,6,7). Clearly, obtaining more information about the mechanisms that control ribonucleotide reductase gene expression is important for understanding the processes of DNA synthesis, DNA repair and cell proliferation (2,3,5).

The regulation of mRNA stability has emerged as an important control mechanism of gene expression. The altered stability of mRNAs is regulated by interactions among *trans*-acting factors (regulatory proteins) and specific sequences (*cis* elements) located mainly within the 3'-UTRs of some mRNAs (8-14). Growth factors such as TGF-β₁ exert their effects by binding to specific cell surface receptors (15,16), and altering the expression of a discrete set of genes important for the regulation of a variety of characteristics, including DNA synthesis and cell proliferation (4,17–20). These TGF-β₁ effects on gene expression may be mediated, at least in part, post-transcriptionally through message stability alterations (21-25). In this regard, transcripts that are preferentially stabilized by TGF-β₁ treatment could contain sequences that are targets for an interaction with a putative TGF-β₁ responsive factor. Most recently we have demonstrated that the TGF-β₁ increased elevation in R2 mRNA levels (3), is at least partly due to the stabilization of R2 mRNA, mediated by a

83 nt fragment of the 3'-UTR (8). This 83 nt fragment, when transcribed into mRNA was shown to form RNA–protein complexes with cytoplasmic extract. *In vitro* decay reactions that contained the 83 nt RNA or deletion of this fragment caused a significant decrease in the TGF-β_1 stabilization of R2 message (8). Although much is now known about DNA sequence elements and transcriptional factors involved in TGF-β_1 transcriptional regulation (e.g. 26–28), there is relatively little information about the mechanism(s) of TGF-β_1 mediated stability of mRNAs. We hypothesized that increased stability of mRNAs in the presence of TGF-β_1 is mediated by the interaction of a cytoplasmic protein(s) *in trans* with a *cis*-element domain(s) within the 3'-UTR.

MATERIALS AND METHODS

Cell culture

Mouse BALB/c 3T3, monkey Cos7, C1, C2 and C3 fibrosarcomas, and Hela S3 cells were routinely cultured in a minimal essential medium (α-MEM) supplemented with antibiotics and 10% (v/v) fetal bovine serum (29). For investigating TGF-β_1 effects on RNA levels and RNA–protein binding activity, cells were grown overnight in a defined medium which was serum-free and contained 0.4 mg transferrin and 0.2 mg insulin (Sigma) in 100 ml α-MEM (3). TGF-β_1 (R and D Systems Inc., Minneapolis, MN) was dissolved in 1.0 mg/ml bovine serum albumin (BSA), and 4 mM hydrochloric acid (HCl) was added at predetermined times. The control plates received 1.0 mg/ml bovine serum albumin (BSA), 4 mM HCl, 0.4 mg transferrin and 0.2 mg insulin in the serum-free medium. The cells were harvested from the tissue culture plates with 0.3% buffered trypsin solution after centrifugation, washed once in phosphate buffered saline (pH 7.2) and transferred to Eppendorf tubes.

Preparation of protein extracts from cytosol, nucleus and salt-extracted polysomes

Cells transferred to Eppendorf tubes were briefly centrifuged for 1 min, and resuspended in hypotonic buffer (25 mM Tris–HCl, pH 7.9, 0.5 mM EDTA) and lysed by repetitive cycles of freeze–thaw. Nuclei were removed by centrifugation at 15,000 g for 5 min in an Eppendorf microcentrifuge, and cytoplasmic extracts were immediately frozen on dry ice and stored at –70°C. The nuclei were extracted for 40 min at 4°C on a rocker in a buffer containing 20 mM HEPES (pH 7.9), 0.53 M HCl, 1.25 mM MgCl$_2$, 0.3 mM EDTA, 0.5 mM dithiothreitol (DTT), 0.5 mM phenylmethylsulfonyl fluoride (PMSF) and 20% glycerol. This nuclear extract mixture was spun at 14,000 g for 10 min in an Eppendorf microcentrifuge, and the supernatants were dialyzed against a solution containing 20 mM HEPES (pH 7.9), 0.1 M KCl, 0.2 mM EDTA, 0.5 mM DTT, 0.5 mM PMSF and 20% glycerol. The nuclear extracts were frozen on dry ice and stored at –70°C (9). Salt-extracted polysomal fractions were obtained as previously described (30), by resuspending the harvested cells in homogenization buffer, 10 mM HEPES (pH 7.6), 0.25 M sucrose, 5 mM MgCl$_2$, 1 mM DTT, 0.1 mM EGTA [ethylene glycol bis (β-aminoethyl ether)-N,N,N',N'-tetraacetic acid], 200 U/ml RNasin (Promega), and protease inhibitors (50 mg/ml of leupeptin and 1 mg/ml of pepstatin) and lysed by repetitive cycles of freeze–thaw. The homogenate was centrifuged for 5 min at 4°C at 700 g. The supernatant was then sedimented by centrifugation (9000 g for 2 min at 2°C and then 100 000 g for 16 min at 2°C). The supernatant

was discarded. The cell pellet was resuspended in homogenization buffer and the centrifugation step was repeated. The crude polysomal pellet was then resuspended in the salt extraction buffer (10 mM Tris–HCl [pH 7.6], 2.5 mM magnesium acetate, 500 mM KCl, 1 mM DTT, 200 U RNasin and protease inhibitor), and incubated for 15 min on ice. The homogenate was diluted with 1 or 2 vol of the buffer described above with KCl and centrifuged at 300 000 g for 60 min at 2°C. The supernatant was aliquoted and stored at –70°C. The protein concentrations of the cytosolic, nuclear and polysomal extracts were determined by the BioRad protein assay kit as described by BioRad (Technical Bulletin 1051), with bovine serum albumin as a standard.

In vitro transcription

A summary of the construction of the *in vitro* transcription plasmid p3'-UTR5 containing the 83 nt *Eco*RI–*Sau*I fragment (nucleotide positions 1861–1944) of mouse R2 3'-UTR cDNA has been previously described (8). In brief, run-off RNA transcripts were produced by T7 polymerase activity (Boehringer Mannheim) from 1 μg of digested cDNA plasmids, in the presence of 40 mM Tris–HCl [pH 7.9], 6 mM MgCl$_2$, 2 mM spermidine, 0.4 mM ribonucleotides (rNTPs), 40 U RNasin and 1 mM DTT for 60 min at 37°C. Two units of RNase free DNase was added, followed by further incubation for 15 min. To produce radiolabeled RNA transcripts, unlabeled CTP was reduced to 25 mM and [α-^{32}P]CTP (3000 Ci/mmol, Amersham Corp.) was added. RNA transcripts were produced as previously described (31), to a specific activity of ~3 × 10^8 c.p.m./mg of RNA. The transcripts were extracted with phenol/chloroform and precipitated with ice cold ethanol, 2.5 M ammonium acetate and *E.coli* tRNA (20 μg/ml). Transcripts were then purified using 15% 8 M urea–polyacrylamide gel. After electrophoresis, the gels were exposed to a Kodak X-Omat AR film for 1 min; the corresponding band was excised and eluted overnight in a solution containing 2 M ammonium acetate and tRNA (25 μg/ml). The eluted mRNA probes were precipitated with ethanol and reconstituted in RNase free water (32), and maintained at –70°C.

3' end-labeling of synthetic RNA oligoribonucleotides

The RNA oligoribonucleotides purchased (Dalton Chemical Laboratories Inc., Toronto, Canada) were synthesized on the Applied Biosystems (ABI) model 392 DNA/RNA synthesizer using phosphoramidite RNA monomers according to the manufacturer's instructions, in User Bulletin no. 47 (ABI). The ribonucleotides were labeled at their 3' ends by a previously described method (33). Briefly oligoribonucleotides were 3'-end labeled by adding successively 10 μl of cytidine 3',5'-[5-^{32}P] biphosphate ([^{32}P]pCp) (Amersham Corp.), 3 μl of 10 × ligase buffer, 3 μl of dimethylsulfoxide, 3 μl of 33 μM ATP (pH 7.0), 5 μg dephosphorylated RNA and 4 U T4 RNA-ligase in a total volume of 30 μl. The reaction mixtures were incubated at 4°C overnight. The labeled RNAs were then phenol/chloroform extracted and precipitated with 2.5 M ammonium acetate, RNA (25 μg/ml) and ice-cold ethanol. The 3' end-labeled RNA oligoribonucleotides were gel purified on 25% 8 M urea–polyacrylamide gels. The RNA bands were visualized by autoradiography and were excised and eluted in 2.5 M ammonium acetate, 0.1% sodium dodecyl sulphate, 5 mM EDTA overnight at 37°C. The RNAs were extracted and reconstituted in RNase free water (32), and stored at –70°C.

RNA mobility shift assay

Ten to forty micrograms of cytosolic, nuclear or polysomal protein extract were incubated with 50×10^3 c.p.m. of ^{32}P-labeled RNA transcript or oligoribonucleotides in 15 mM KCl, 5 mM MgCl$_2$, 0.25 mM EDTA, 0.25 mM DTT, 12 mM HEPES (pH 7.9), 10% glycerol and *E.coli* tRNA (200 ng/ml) in a total volume of 10 μl at 30°C for 60 min (31). Fifty units of RNase T$_1$ (Boehringer Mannheim) were added when the R2 3'-UTR was used (but not for binding reactions with the 3' end-labeled oligoribonucleotides), and the reaction mixtures were incubated at 37°C for 30 min. To remove non-specific protein binding, when the R2 3'-UTR or 83 nt was used, 5 mg/ml heparin was added and the mixture was incubated on ice for an additional 10 min. Samples were then subjected to electrophoresis in a 7–15% native polyacrylamide gel with 0.25 × TBE (Tris–borate–EDTA) running buffer. The gels were dried and exposed to Kodak X-Omat AR films at –70°C. In some assays cytoplasmic extracts were pre-incubated with compounds, such as proteinase K for 10 min, before addition of the riboprobe.

UV cross-linking analyses

RNA–protein binding reactions were carried out as described above using 10–40 μg of cytosolic protein extract and 10×10^4 c.p.m. of labeled riboprobe per reaction. Following the addition of heparin, samples were placed in microtitre wells placed on ice and irradiated for 10 min in a Stratalinker Chamber (Stratagene), a UV cross-linking apparatus, at 250 mJ (energy level). The samples were then boiled in Laemmli sample buffer and separated by electrophoresis on a 10% SDS–polyacrylamide gel (31). The gels were dried and exposed to Kodak X-Omat AR films at –70°C. The bands visualized in the autoradiographs of the RNA-binding gel shift and UV-cross-linking assays were sometimes more diffuse and not as sharp as, for example, the same assays performed with a DNA probe. This is primarily due to the structural complexity of single-stranded RNA when it is subjected to non-denaturing gel electrophoresis. In addition, it is possible the RNA–protein complexes dissociate to some degree during electrophoresis resulting in a more diffuse banding pattern (34).

RESULTS

Identification of a novel *cis* element in the 3'-UTR

To identify the sequence within the 83 nt R2 3'-UTR fragment that forms the RNA–protein complexes, previously shown to contain information for R2 mRNA stabilization (8; Fig. 1), we generated a series of synthetic oligoribonucleotides: 5'-AAUUCAAGU-GAG, GAGUUUGAG, CCCAGUGGUGUA, CACCCGUGGG, ACUCUCUUAC, AAACCAAAACA, GGAAAA GCAA, GU-GUUUCCC-3' corresponding to different segments of the 83 nt RNA fragment. The data, summarized in Figure 1A, indicates the region for protein binding observed in RNA gel shift assays, performed with a series of smaller segments of 3' end-labeled oligoribonucleotides corresponding to different regions of the 83 nt fragment (Fig. 1B). The data indicated that the 9 nt region 5'-GAGUUUGAG-3' is the binding site for the protein within the R2 3'-UTR (Fig. 1B), shown by the formation of two major RNA–protein complex band shifts, when the *cis* element and R2 3'-UTR RNA probes were incubated with cytoplasmic extracts from 10 ng/ml TGF-β$_1$ treated mouse BALB/c 3T3 fibroblasts
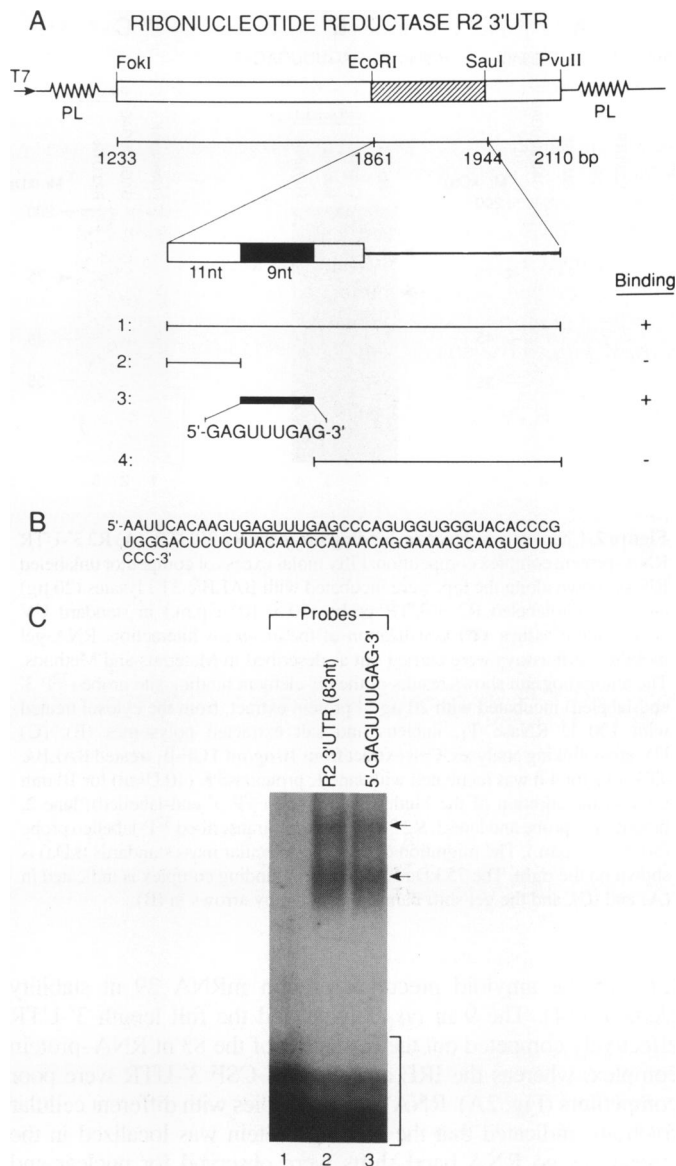
Figure 1. Identification of the protein binding site in mouse ribonucleotide reductase R2 mRNA. (**A**) Schematic diagram of the 3'-UTR of R2 mRNA is shown at the top of (A). The T7 promoter used to generate the R2 3'-UTR (83 nt probe) is indicated, and the region of the polylinker (PL) is shown. The 3'-UTR shown as a striped fragment (83 nt probe) has been subdivided into smaller segments of ^{32}P 3' end-labeled synthetic oligoribonucleotides with the indicated lengths (nt). Lane 1, the 83 nt fragment; lane 2, the first fragment of 11 nt; lane 3, the 9 nt *cis* element and lane 4, sequences downstream of the *cis* element. The RNA–protein binding characteristics are indicated at the right as no detectable binding (–) to detectable binding (+). (**B**) Shows the 83 nt sequence containing the *cis* element (underlined) of the R2 3'-UTR that binds the TGF-β$_1$ responsive protein. (**C**) Shows gel shift assays using the 83 nt R2 3'-UTR fragment (50×10^3 c.p.m.) incubated with protein extracts from 10 ng/ml TGF-β$_1$, untreated and treated BALB/c 3T3 mouse fibroblasts for 4 h (lanes 1 and 2, respectively) and the *cis* element, GAGUUUGAG riboprobe incubated with 30 μg of protein extract from 10 ng/ml TGF-β$_1$ treated mouse BALB/c 3T3 fibroblasts. The RNA–protein shift complex bands are indicated by the arrows, while free digested RNA (in the case of R2 3'-UTR) or free 3' end-labeled probes are bracketed in all the figures, unless otherwise stated.

(Fig. 1C). The 9 nt *cis* element appears to be unique, as it does not resemble any known, previously described RNA *cis* element, such as the AU-rich pentamer (11), the iron response element (IRE) (35), the ornithine decarboxylase 5'-UTR conserved sequence
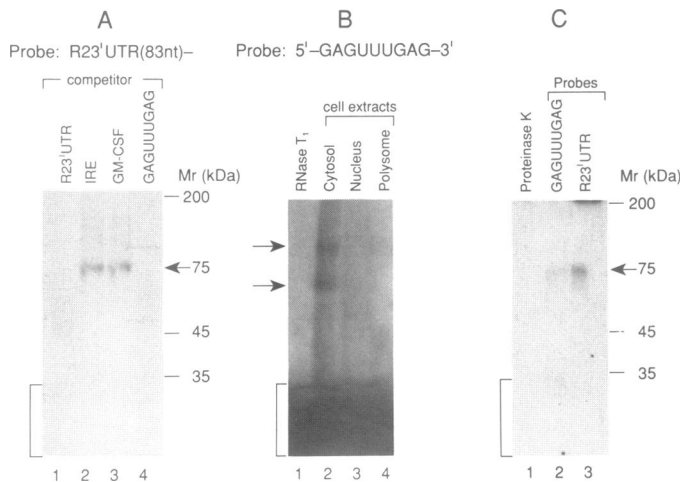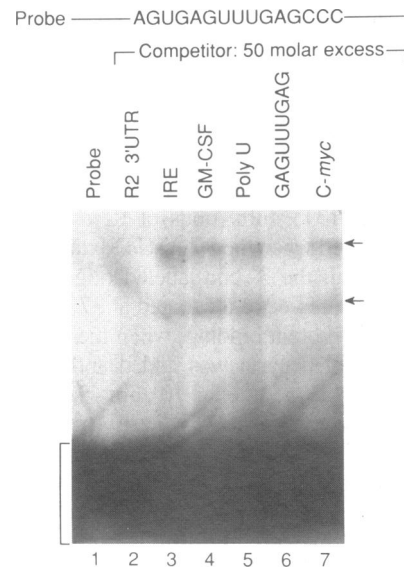
Figure 2. Characterization of the binding site in the R2 3′-UTR. (A) R2 3′-UTR RNA–protein complex competition. Fifty molar excess of competitor unlabeled RNAs shown along the top, were incubated with BALB/c 3T3 lysates (20 μg) and ^{32}P-radiolabeled R2 3′-UTR probe (50 × 10^3 c.p.m.) in standard UV cross-linking assays. (B) Localization of the *cis–trans* interaction. RNA gel mobility shift assays were carried out as described in Materials and Methods. The autoradiogram shows results of the *cis*-element binding site probe (^{32}P 3′ end-labeled) incubated with 20 μg of protein extract, from the cytosol treated with 100 U RNase T_1, nucleus and salt extracted polysomes (B). (C) UV-cross-linking analyses. Cell extract from 10 ng/ml TGF-β$_1$ treated BALB/c 3T3 cells for 4 h was incubated with lane 1: proteinase K (40 U/ml) for 10 min prior to the addition of the binding site probe (^{32}P 3′ end-labelled); lane 2, binding site probe and lane 3, R2 3′-UTR *in vitro* transcribed ^{32}P-labelled probe (50 × 10^3 c.p.m.). The migration of protein molecular mass standards (kDa) is shown on the right. The 75 kDa RNA–protein binding complex is indicated in (A) and (C), and the gel shift bands are shown by arrows in (B).


Figure 3. Binding specificity of the R2 mRNA binding site. Autoradiogram of RNA gel shift assays performed in the presence of ^{32}P 3′ end-labeled oligoribonucleotide (5′-AGUGAGUUUGAGCCC-3′; 50 × 10^3 c.p.m.) shown along the top. Lane 1, probe alone; lane 2, RNA mobility shift competition assays with 50 molar excess of unlabelled R2 3′-UTR; lane 3, 50 molar excess of the iron response element; lane 4, 50 molar excess of the GM-CSF 3′-UTR; lane 5, 50 molar excess of the homopolymer (U); lane 6, 50 molar excess of the 9 nt *cis* element; lane 7, 50 molar excess of the c-*myc* 3′-UTR. The above were incubated in the presence of 20 μg of BALB c/3T3 protein extract. The cells were treated for 6 h with 10 ng/ml TGF-β$_1$. The arrows indicate the position of the gel shift bands clearly visible in lanes 3, 4, 5 and 7.

(36), or the amyloid precursor protein mRNA 29 nt stability element (14). The 9 nt *cis* element and the full length 3′-UTR effectively competed out the formation of the 83 nt RNA–protein complex, whereas the IRE and the GM-CSF 3′-UTR were poor competitors (Fig. 2A). RNA binding studies with different cellular fractions, indicated that the binding protein was localized in the cytosol, as no RNA band shifts were observed for nuclear and polysomal extract (Fig. 2B, lanes 2, 3 and 4, respectively). Pre-treatment of the cytosolic extract from TGF-β$_1$ treated cells with RNase T_1 totally inhibited the formation of the RNA–protein complex (Fig. 2B, lane 1). Pre-treatment with Proteinase K of cytosolic extract from BALB/c 3T3 cells treated with 10 ng/ml TGF-β$_1$, abolished the formation of the 75 kDa UV-cross-linked RNA–protein migration band observed for the 9 nt *cis* element and the 83 nt fragment (Fig. 2C, lane 1). In the absence of proteinase K treatment, the TGF-β$_1$ dependent migration band was observed with both the 9 nt sequence and the R2 3′-UTR (Fig. 2C, lanes 2 and 3). These results indicate that the complex detected in these experiments is composed of RNA and polypeptides.

Specificity and kinetics of the *cis*-element binding activity

The localization of the binding site (5′-GAGUUUGAG-3′) to a small portion of the R2 3′-UTR strongly suggested that binding of the protein to the 9 nt sequence occurred with a high degree of specificity. This was tested further in competition gel shift assays. A ^{32}P 3′ end-labelled 15 nt R2 3′-UTR riboprobe was used, which exhibited binding to the putative TGF-β$_1$ response protein. We

compared the abilities of the unrelated mRNAs, IRE, the 3′-UTR of c-*myc*, the 3′-UTR of GM-CSF and the homopolymer (U) to compete with the 15 nt in binding experiments (Fig. 3). The R2 3′-UTR and the 9 nt *cis* element prevented formation of the RNA–protein complexes, but in contrast, the 3′-UTRs of c-*myc* and GM-CSF, the IRE and the homopolymer (U) were very poor competitors. UV-cross-linking analyses of cytosolic extracts from BALB/c 3T3 cells with the 9 nt *cis* element showed that the RNA binding activity was markedly elevated within 4 h post TGF-β$_1$ treatment, compared to untreated cell lysates. Binding activity was investigated in the presence of increasing concentration of cytosolic extract from cells treated with TGF-β$_1$ incubated with the 9 nt *cis* element probe (Fig. 4B). The binding to labelled RNA increased with each increase in protein concentration between 5 and 20 μg of cytosolic protein. Similarly, in control experiments, a protein concentration dependent increase in binding activity was also observed in these experiments with labelled AU-rich GM-CSF 3′-UTR (Fig. 4B).

Effect of mutations on the *cis* element-protein binding activity

The effects of various mutations within the protein binding *cis*-element (5′-GAGUUUGAG-3′) site were assessed by monitoring the formation of the major RNA–protein complex band shifts under standard gel shift assays. Figure 5A and B indicates the bases (underlined) that have been changed from the wild type sequence. Mutations within this *cis* element disrupted binding (Fig. 5A). For example, mutations of any one of the core three U residues to an A, C or G residue abolished binding activity (Fig.
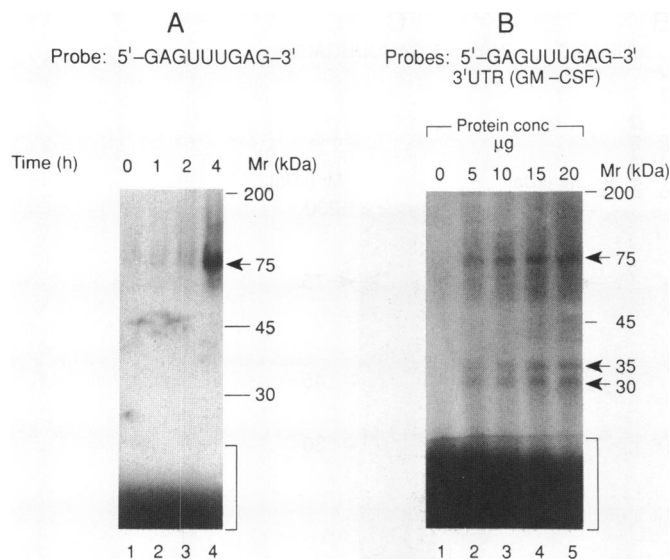
Figure 4. TGF-β₁ mediated R2 mRNA–protein binding. (**A**) 40 μg of cytosolic protein extract from BALB/c 3T3 cells treated with 10 ng/ml TGF-β₁ for the pre-determined times (h) indicated along the top were incubated with the *cis* element ^{32}P 3′ end-labeled probe (50 × 10³ c.p.m.) in UV-cross-linking analyses. (**B**) A representative autoradiogram of an RNA UV cross-linking analyses using the 9 nt *cis* element and GM-CSF (human) 3′-UTR mRNA probe incubated with increasing concentration of protein extract (0–20 μg) from TGF-β₁ treated BALB/c 3T3 cells for 4 h. Following successive incubations with heparan sulphate to remove non-specific binding, the reaction mixtures were UV-cross-linked on a Stratalinker cross-linking apparatus and were separated by electrophoresis on 10% SDS–PAGE. The migration of protein molecular mass standards (kDa) is shown on the right. Arrows indicate the positions of the 75 kDa RNA–protein binding complex (A and B) and the GM-CSF 3′-UTR cross-linked 30–35 kDa RNA–protein complexes (B).
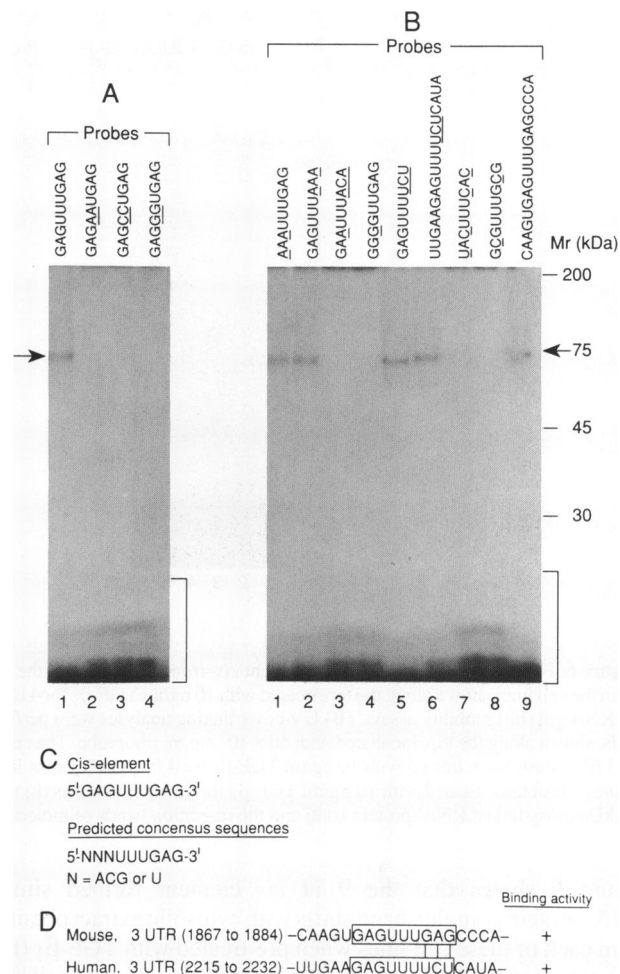

Figure 5. UV-cross-linking analyses of normal and mutant *cis* element probes. RNA UV-cross-linking assays were performed using cytoplasmic extracts (20 μg) from BALB/c 3T3 fibroblasts treated with TGF-β₁ (10 ng/ml) for 4 h. (**A**) The cytoplasmic extract incubated with 50 × 10³ c.p.m. of ^{32}P 3′ end-labeled oligoribonucleotide probe is shown along the top of the autoradiograms. Lane 1, wild type sequence; lanes 2–4, mutant oligoribonucleotides with substitution mutations in the three core U residues to A, C and G residues as shown. (**B**) Substitution mutations in the 5′ or 3′ flanking GAG residues. Lanes 1–9, UV cross-linking results obtained with the sequences indicated at the top of each panel. The various oligoribonucleotides were 3′ end-labelled, and used as probes in RNA gel UV-cross-linking assays. The underlinked bases refer to those changed from the wild-type sequence. (**C**) Sequence of the 9 nt *cis*-element binding site identified in the 3′-UTR of R2 mRNA, that interacts with a putative TGF-β₁ inducible *trans*-factor. (**D**) Comparison of the TGF-β₁ dependent *trans*-factor binding sites from selected R2 cDNA clones of mouse mammary tumor cells (38), and human breast carcinoma cells (37). Sequences were aligned, and the *cis* elements are boxed. The vertical lines represent nucleotide substitutions and the numbers in brackets indicate the positions of the nucleotides.

5A). Replacement of either G residues within this motif also abolished binding. Mutations of three consecutive bases of either the 5′ or 3′ GAG flanking residues did not prevent binding, for example AAAUUUGAG or GAGUUUAAA or GAGUUUUCU (Fig. 5B, lanes 1, 2 and 5). However, mutations in both of the GAG motifs flanking the core U residues dramatically decreased binding activity, for example GAAUUUACA and UACUUUC-AC (Fig. 5B, lanes 3 and 7). In addition, mutation of the single A residue within the GAG motifs also abolished binding (Fig. 5B, lanes 4 and 8). Due to the lack of preference in these binding experiments for either of the GAG flanking motifs (although at least one must be present), and the importance of the core U residues, the following consensus *cis* element sequence is suggested for the optimal binding to the TGF-β₁ responsive protein(s): 5′-GAGUUUNNN-3′ and 5′-NNNUUUGAG-3′. In support of this proposal is the observation that the sequences 5′-UUGAAGAGUUUUCUCAUA-3′ and 5′-CAAGUGAGUU UGAGCCCA-3′, which showed TGF-β₁ inducible RNA–protein binding activities (Fig. 5, lanes 6 and 9) are found at nucleotide positions 2215–2232 in the R2 cDNA cloned from human breast carcinoma (37), and at nucleotide positions 1867–1884 in the R2 cDNA from mouse tumor cells (38).

Cellular and species expression of the *cis* element binding activity

The observation that human and mouse R2 cDNA code for RNA that contains the *cis* element consensus motif described above

prompted us to investigate the possibility that this *cis* element in the R2 mRNA 3′-UTR interacts with similar TGF-β₁ responsive *trans*-factors in other cell types from several different species. Therefore, RNA gel shift assays were performed with 30 μg of protein from cytosolic extracts from BALB/c 3T3 mouse fibroblasts, C1, C2 and C3 mouse fibrosarcoma cells derived from 10T½ cells following T24-H-*ras* transfection (39), human Hela S3 cells and Cos 7 monkey kidney fibroblasts. These cells were pre-treated with 10 ng/ml TGF-β₁ for 4 h or left untreated.
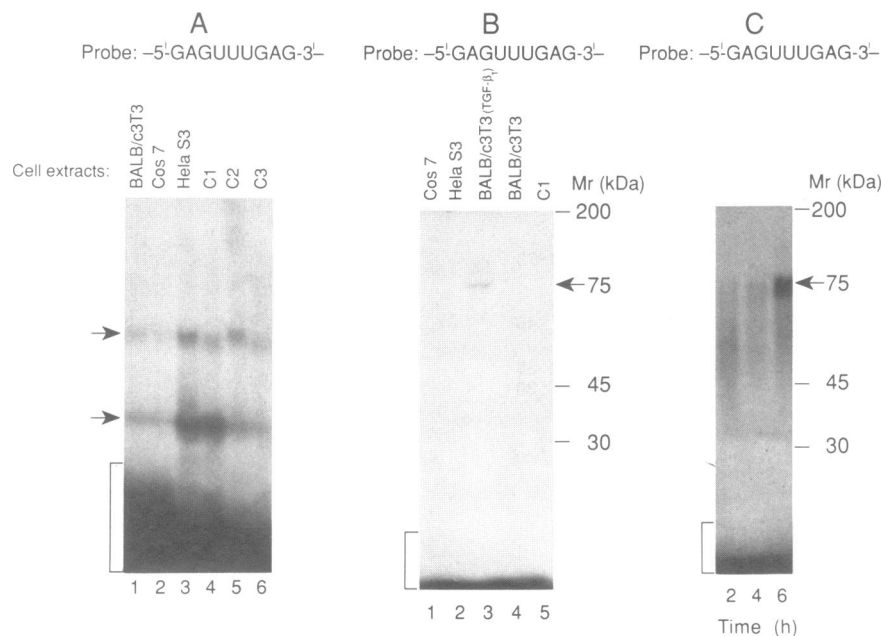
Figure 6. Expression of the TGF-β₁ dependent *cis–trans* interaction at the 3'-UTR of R2 mRNA of a variety of cell lines. (**A**) 20 μg of cytoplasmic protein extract from the cell lines shown along the top, treated with 10 ng/ml TGF-β₁ for 4 h, were incubated with the R2 3'-UTR *cis* element riboprobe (50 × 10³ c.p.m.), and analyzed by RNA gel shift mobility assays. (**B**) UV-cross-linking analyses were performed in the presence of 20 μg of cytoplasmic protein extract from different mammalian cells, shown along the top, incubated with 50 × 10³ c.p.m. riboprobe. The cell extracts were from untreated cells (lanes 1, 2, 4 and 5) except for lane 3, where BALB/c 3T3 fibroblasts were treated with 10 ng/ml TGF-β₁ for 4 h. (**C**) UV-cross-linking analyses performed with 20 μg of cytoplasmic protein extract from Cos 7 monkey kidney fibroblasts, treated with 10 ng/ml TGF-β₁ for the various times (h) indicated at the bottom. The arrows in (A) indicate the RNA mobility band shifts, and the 75 kDa cross-linked RNA–protein band and the migration bands of molecular mass standards (kDa) are shown on the right side of (B) and (C).

Figure 6 shows that the 9 nt *cis* element formed similar RNA–protein complex band shifts with cytosolic extract obtained from each of these cell lines when pre-treated with TGF-β₁ (Fig. 6A), whereas cytosolic extracts prepared from untreated cell lines showed no binding activity in gel shift assays (data not shown) or in UV-cross-linking analyses (Fig. 6B). These observations suggest that there is an interaction between the 9 nt *cis* element and similar putative TGF-β₁ responsive proteins, that act *in trans* in each of these cell types representing several different species. The time dependent inducibility of the 75 kDa RNA–protein band complex in Cos 7 monkey kidney cells treated with 10 ng/ml TGF-β₁ is shown in Figure 6C.

DISCUSSION

Although much is known about transcriptional mechanisms involved in TGF-β₁ regulation of gene responses (for example, see 26–28), very little is known about the molecular mechanisms leading to TGF-β₁ induction of message stability. We have identified a novel 9 nt *cis* element, 5'-GAGUUUGAG-3' within the R2 mRNA 3'-UTR, which is the binding site for a TGF-β₁ responsive cytosolic protease sensitive *trans*-acting factor(s). The *cis* element protein complex was UV cross-linked to form a 75 kDa complex migration band, similar to results obtained from experiments with the 83 nt R2 3'-UTR fragment (8). Sequences flanking the *cis* element in the 3'-UTR may modulate the affinity of protein binding by affecting RNA structures, for example, stem–loop secondary structures, which are a common feature of RNA binding sequences (40,41). The inducible binding activity of the *cis* element represented a sequence specific interaction because, RNA–protein band shifts were not abolished in the presence of unrelated competitors, like ribohomopolymer

poly(U), the IRE and other mRNA 3'-UTRs (GM-CSF and c-*myc*). In contrast, addition of the 9 nt *cis* element efficiently competed for protein binding to the R2 3'-UTR 83 nt fragment. The TGF-β₁ responsive protein interaction with the R2 3'-UTR *cis* element fragment showed similar binding characteristics in a variety of cells of different species suggesting a common pathway of TGF-β₁ induced stabilization of R2 mRNA.

Similar to several previously published mRNA *cis* elements (31,36,42,43), there is only one copy of the 9 nt *cis* element within the R2 message. The mutagenesis studies summarized in Figure 5 indicated that there are relatively stringent primary sequence requirements for optimum protein binding. We predict that the consensus motifs for optimal binding activity with a TGF-β₁ responsive protein are 5'-GAGUUUNNN-3' and 5'-NNNUUU-GAG-3'. A computer search for the consensus motifs revealed the presence of similar sequences. For example, human R2 mRNA contained the sequence motif; 5'-GAGUUUUCU-3' which showed identical TGF-β₁ responsive RNA–protein band shifts as the mouse sequence (5'-GAGUUUGAG-3'). Knowledge of a consensus RNA binding motif for TGF-β₁ responsive mRNA stabilizing protein may alert us to regulatory sequences present in candidate mRNAs, such as for example, α1(I) collagen mRNA (22). The precise role of these sequences in binding must, however, await detailed analysis of the contribution of individual nucleotides, since binding may involve both primary sequences and secondary structures (44). While we cannot directly relate features of the binding site to the still unknown pathway of degradation of R2 mRNA, it is noteworthy that the 9 nt *cis* element region is flanked by AAU and GUGGUG sequences, previously described as initial cleavage sites in single-stranded loops in 3'-UTR sequences (45). The location of the *cis* element

in the region of a 3'-UTR with a potential cleavage site flanking the protein binding site is consistent with what is known about the regulation of mRNA stability, which is thought to function by repressing the activity of mRNA destabilizing sequences (44,46,47). It is notable that other segments of the 3'-UTR, excluding the binding site, do not exhibit TGF-β_1 responsive protein binding activity, however, our results do not rule out the possibility and even the likelihood that flanking and proximal 3'-UTR sequences may also play a role in determining optimal message stability characteristics. For example, a 3'-UTR 39 base uridine-rich domain adjacent to the AUUUA motif is critical for mediating rapid c-*myc* message degradation (48), as well as sequences in the C-terminal portion of the c-*myc* coding region (49). Among the questions that remain to be further investigated, several concern potential mechanisms by which TGF-β_1 could induce a responsive protein, and the regulation of its interaction with the 9 nt *cis* element. Several possibilities exist. For example, activation by TGF-β_1 may be mediated by a protein whose RNA binding properties are affected by phosphorylation. Such a mechanism has recently been proposed for the post-transcriptional regulation of ribonucleotide reductase R1 gene expression, through a specific 3'-UTR *cis–trans* interaction that is sensitive to treatment with the tumor promoter, 12-0-tetradecanoylphorbol-13-acetate, and is controlled through a protein kinase C pathway (32). Similarly, the cytoplasmic redox state of an RNA binding protein through a 'sulfhydryl switch' has been shown to influence the interaction of proteins with mRNA (34), and it is possible that this process could be growth factor responsive.

In summary, the localization of the 9 nt *cis* element to the 3'-UTR and the specificity and inducibility of the binding activity support the view that the *cis* element we have identified plays a critical role in the TGF-β_1 induced stability of R2 mRNA. The results are consistent with a model in which the 9 nt region functions *in cis* to destabilize R2 mRNA in cells, and the TGF-β_1 responsive protein(s) interacts with the 9 nt region, which is directly linked to a mechanism that reduces the rate of R2 mRNA degradation. Whatever the precise function of the *cis* element, it represents the first example of a class of TGF-β_1 responsive *cis* elements in the 3'-UTR of mRNAs.

ACKNOWLEDGEMENTS

REFERENCES

1 Wright, J.A. (1989). *Int. Encyclop. Pharmacol. Therapeut.*, **128**, 89–111.
2 Wright, J.A., Chan, A.K., Choy, B.K., Hurta, R.A.R., McClarty, G.A. and Tagger, A.Y. (1990). *Biochem. Cell Biol.*, **68**, 1364–1371.
3 Hurta, R.A.R., Samuel, S.K., Greenberg, A.H. and Wright, J.A. (1991). *J. Biol. Chem.*, **266**, 24097–24100.
4 Wright, J.A., Turley, E.A. and Greenberg, A.H. (1993). *Crit. Rev. Oncogenesis*, **4**, 473–492.
5 Hurta, R.A.R. and Wright, J.A. (1992). *J. Biol. Chem.*, **267**, 7066–7071.
6 Weber, G. (1983). *Cancer Res.*, **43**, 3466–3492.
7 Juliusson, G. and Liliemark, J. (1993). *J. Clinical Oncology*, **11**, 679–689.
8 Amara, F.M., Chen, F.Y. and Wright, J.A. (1993). *Nucleic Acids Res.*, **21**, 4803–4809.
9 Amara, F.M., Chen, F.Y. and Wright, J.A. (1994). *J. Biol. Chem.*, **269**, 6709–6715.
10 Chen, F.Y., Amara, F.M. and Wright, J.A. (1993). *EMBO J.*, **12**, 3977–3986.
11 Brewer, G. (1991). *Mol. Cell Biol.*, **11**, 2460–2466.
12 Bohjanen, P.R., Petryniak, B., June, C.H., Thompson, C.B. and Lindsten, T. (1991). *Mol. Cell. Biol.*, **11**, 3288–3295.
13 Zaidi, S.H.E. and Malter, J.S. (1994). *J. Biol. Chem.*, **269**, 24000–26000.
14 Zaidi, S.H.E., Denman, R. and Malter, J.S. (1994). *J. Biol. Chem.*, **269**, 24007–24013.
15 Kataoka, R., Sherlock, J. and Lanier, S.M. (1993). *J. Biol. Chem.*, **268**, 19851–19857.
16 Wrana, L.J., Ahisano, L., Wieser, R., Ventura, F. and Massague, J. (1994). *Nature*, **340**, 341–347.
17 Loef, E.B., Proper, J.A., Gouslin, A.S., Shipley, G.D., DiCorlets, P.E. and Moses, H.L. (1986). *Proc. Natl. Acad. Sci. USA*, **83**, 2453–2457.
18 Schwarz, L.C., Gingras, M.-C., Goldberg, G., Greenberg, A.H. and Wright, J.A. (1988). *Cancer Res.*, **48**, 6999–7003.
19 Schwarz, L.C., Wright, J.A., Gingras, M.C., Kondaiah, P., Danielpour, D., Pimentel, M., Sporn, M.B. and Greenberg, A.H. (1990). *Growth Factors* **3**, 115–127.
20 Roberts, A.B. and Sporn, M.B. (1990). In, *Handbook of Experimental Pharmacology.* Eds, Springer Verlag Heidelberg, 419–472.
21 Matrisian, L.M., Leroy, P., Ruhlman, C., Gesnel, M.C. and Breuthnach, R. (1986). *Mol. Cell. Biol.*, **6**, 1679–1686.
22 Penttinen, R.P., Kobayashi, S. and Bornstein, P. (1988). *Proc. Natl. Acad. Sci. USA*, **85**, 1105–1108.
23 Rossi, P., Karsenty, G., Roberts, A.B., Roche, N.S., Sporn, M.B., deCrombrugghe, B. (1988). *Cell*, **52**, 405–514.
24 Overall, C.M., Jeffrey, L., Wrana and Sodek, J. (1991). *J. Biol. Chem.*, **266**, 14064–14071.
25 Hurta, R.A.R. and Wright, J.A. (1994). *J. Cell. Biochem.*, **57**, 543–556.
26 Kerr, L.D., Miller, D.B. and Matrisian, L.M. (1990). *Cell*, **51**, 267–278.
27 Moses, H.L., Yang, E.Y. and Pietenpol, J.A. (1990). *Cell*, **63**, 245–247.
28 Roberts, A.B., Kim, S., Noma, T., Glick, A.B., Lafyatis, R., Lechleider, R., Jackondew, S.B., Gerser, A., O'Reilly, M.A., Danielpour, D. and Sporn, M.B. (1991). *Ciba Found. Symp.* **157**, 7–28.
29 Blosmanis, R., Wright, J.A. and Goldenberg, G.J. (1987). *Cancer Res.*, **47**, 1273–1277.
30 Dodson, R.E. and Shapiro, D.J. (1994). *Mol. Cell Biol.*, **14**, 3130–3138.
31 Rondon, I.J., MacMillan, L.A., Beckman, B.S., Boldberg, M.A., Schneider, T., Bunn, H.F. and Malter, J.S. (1991). *J. Biol. Chem.*, **266**, 16594–16598.
32 Chen, F.Y., Amara, F.M. and Wright, J.A. (1994). *Biochem. J.*, **302**, 125–132.
33 Bruce, A.G. and Uhlenbeck, O.C. (1976). *Nucleic Acids Res.* **5**, 3665–3677.
34 Clerch, B.L. and Massaro, D. (1992). *J. Biol. Chem.*, **267**, 2853–2855.
35 Leibold, E.A. and Munro, H.N. (1988). *Proc. Natl. Acad. Sci. USA*, **85**, 2171–2175.
36 Manzella, J.M. and Blackshear, P.J. (1992). *J. Biol. Chem.*, **267**, 7077–7082, 1992.
37 Pavloff, N., Rivard, D., Masson, S., Shen, H.–S. and Marron, Mes., M.A. (1992) *J. DNA Seq. Map*, **2**, 227–234.
38 Thelander, M. and Berg, P. (1986). *Mol. Cell. Biol.*, **6**, 3433–3442.
39 Egan, S.E., McClarty, G.A., Jarolim, L., Wright, J.A., Spiro, I., Hager, G., Greenberg, A.H. (1987). *Mol. Cell. Biol.*, **7**, 830–837.
40 Koeller, D.M., Horowitz, J.A., Casey, J.L., Klausner, R.D. and Harford, J.B. (1991). *Proc. Natl. Acad. Sci. USA*, **88**, 7778–7782.
41 Burd, C.G. and Dreyfuss, G. (1994). *Science*, **265**, 615–621.
42 Casey, J.L., DeJeso, B., Rao, K., Klausner, R.D. and Harford, J.B. (1988). *Proc. Natl. Acad. Sci. USA*, **85**, 1787–1791.
43 Sachs, A.B. (1993). *Cell*, **74**, 413–421.
44 Klausner, R.D., Roualt, T.A. and Harford, J.B. (1993). *Cell*, **72**, 19–28.
45 Binder, R.S.L., Wang, R., Ratnasabapathy, R. and Williams, D.L. (1989). *J. Biol. Chem.*, **264**, 16910–16918.
46 Malter, J.S. (1989). *Science*, **246**, 664–666.
47 Heaton, B., Decker, C., Muhlrad, D., Donahue, J., Jacobson, A. and Parker, R. (1992). *Nucleic Acids Res.*, **20**, 5365–5373.
48 Alberta, J.A., Rundell, K. and Stiles, C.D. (1994). *J. Biol. Chem.*, **269**, 4532–4538.
49 Prokipcak, R.D., Herrick, D.J. and Ross, J. (1994). *J. Biol. Chem.*, **269**, 9261–9269.